J Nanostruct 16(3): 4057-4066, Summer 2026

RESEARCH PAPER

Preparation and Characterization of Green Chitosan Nanocomposites and Evaluation of Their Inhibitory Role Against Certain Gram-Negative Bacteria

Israa Saheb Radhi *, Kiaser Abdalsajjad M. Hussain

Department of Biology, College of Education for pure Sciences, University of Kerbala, Karbala, Iraq

ARTICLE INFO

Article History:
Received 09 April 2026
Accepted 20 June 2026
Published 01 July 2026

Keywords:
AFM
Chitosan
G-negative bacteria
Nanocomposite
SEM

ABSTRACT

This study sought to diagnose the types of bacteria causing urinary tract infections (UTI) in pregnant women and women who have had abortions. Recurrent miscarriage is a serious health problem, often associated with bacterial infections, particularly those caused by Gram-negative bacteria. The emergence of antibiotic resistance among pathogenic bacteria has spurred the development of new treatment approaches based on nanotechnology. This study also investigated antibiotic resistance patterns and the efficacy of environmentally friendly chitosan nanoparticles, evaluating their effectiveness against Gram-negative bacterial isolates before and after loading them with the antibiotic cefotaxime (CTX). The isolates included *Escherichia coli, Klebsiella enterica*, and *Pseudomonas aeruginosa.* exhibited resistance to many antibiotics and sensitivity to others. bacterial isolates were extracted and identified using the VITEK2 system. The surface was characterized by using SEM and AFM techniques. The most prevalent pathogenic bacteria identified were *Escherichia coli* (18 isolates), followed by *Klebsiella* pneumoniae (9 isolates), then *Staphylococcus aureus* and *Pseudomonas aeruginosa*. Antibiotic susceptibility testing revealed high resistance, with *Escherichia coli* exhibiting complete (100%) resistance to cefotaxime (CTX) at a minimum inhibitory concentration (MIC) of ≥ 32 µg/ml.

How to cite this article
Radhi I., Hussain K. Preparation and Characterization of Green Chitosan Nanocomposites and Evaluation of Their Inhibitory Role Against Certain Gram-Negative Bacteria. J Nanostruct, 2026; 16(3):4057-4066. DOI: 10.22052/JNS.2026.03.089

INTRODUCTION

Recurrent miscarriage remains a serious reproductive health problem worldwide. It is defined as two or more consecutive pregnancy losses before the 20th week of gestation. Recurrent miscarriage is a complex and multifactorial reproductive issue. Known causes of recurrent miscarriage include chromosomal abnormalities, uterine malformations, coagulation disorders, metabolic factors, endocrine disorders, autoimmune disorders, as well as lifestyle habits and general health status. [1-3] It affects a significant number of women during their reproductive years. Although anatomical, genetic, immunological, hormonal, lifestyle, and metabolic factors contribute to miscarriage, microbial infections are a major contributing factor to the

* *Corresponding Author Email: asraa.sahib@s.uokerbala.edu.iq*

risk of recurrent miscarriage. [4] Urinary tract infections (UTIs) are among the most common and important diseases affecting women [5,6] UTIs are often associated with multiple pathogens, including Gram-negative bacteria, Gram-positive bacteria, and some fungi, with an annual prevalence of up to 30% among women and 10% among men [7]. The most common causative agent is Escherichia coli, followed by Klebsiella spp. Staphylococcus [8]. Over the past decade, antibiotic resistance has emerged as a health threat, and the overuse and misuse of antibiotics may lead to the development of resistant bacterial strains [9]. The antibiotic cefotaxime has been widely used to treat urinary tract infections, but its resistance has increased among clinical isolates [10]. Nanotechnology has opened a new path for the development of advanced antimicrobial methods. Chitosan has received considerable attention due to its biodegradability

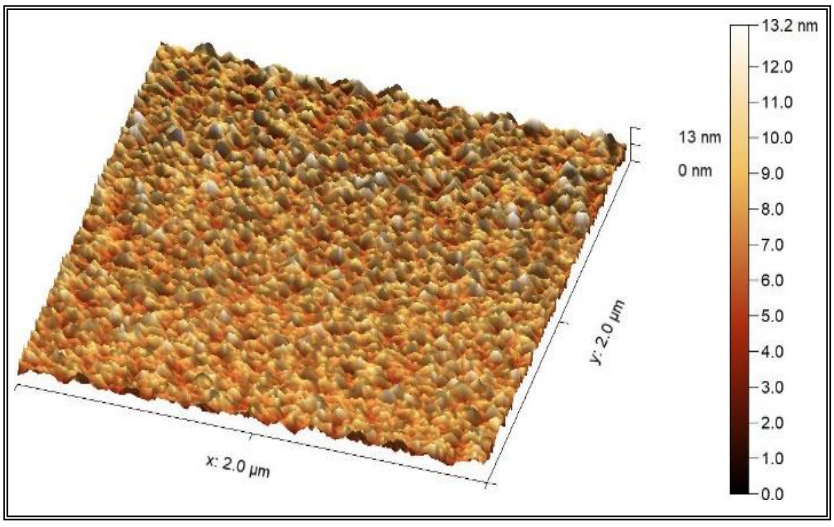

Fig. 1. Atomic force microscope image of CSNPs Nanocomposite showing the highest.

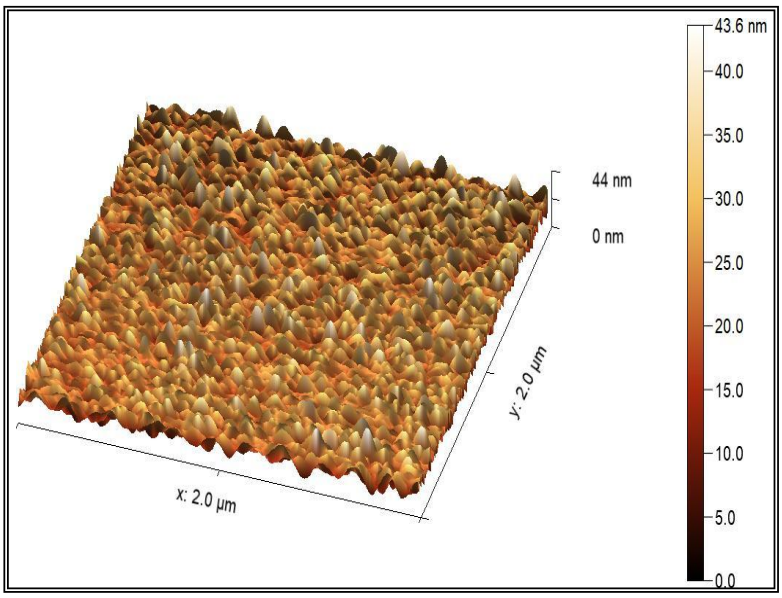

Fig. 2. Atomic force microscope image of the CSNPs/ the antibiotic CTX.

and antimicrobial properties. It is a natural polysaccharide extracted by removing the acetyl group from chitin extracted from shrimp shells [11,12]. Chitosan reacts with negatively charged bacterial cell membranes, leading to membrane rupture and inhibiting bacterial growth [13]. Recent studies have shown that nanotechnology can significantly enhance the biological activity of treatments. Nanotechnology improves antibiotic performance after loading onto nanoparticles [14]. The effectiveness of nanoparticle synthesis is demonstrated in improving biological responses and therapeutic efficacy [15,16]. The importance of nanomaterials derived from natural sources is expected to lead to future advancements in medicine and other industries [17,18]. Based on this, the current study aimed to isolate and identify bacteria causing urinary tract infections (UTI) in women with miscarriages, evaluate antibiotic resistance mechanisms, synthesize chitosan nanoparticles from shrimp shells, and investigate their efficacy before and after loading with the antibiotic cefotaxime (CTX) against resistant bacterial isolates.

MATERIALS AND METHODS

SCTXle Collection

75 clinical urine sampleswere collected

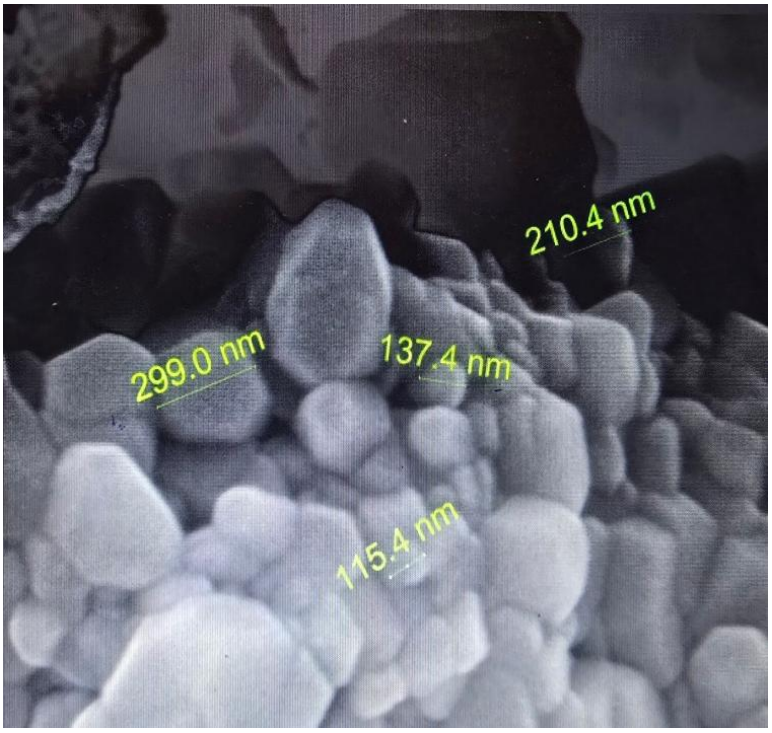

Fig. 3. SEM image showing the morphology nano composite surface.

Table 1. demonstrates the various physical attributes of the free CSNPs nanocomposite comparing their states ahead of and after CTX.

Physical properties of free and loaded nanocomposites	CSNPs(nm)	CTX-CSNPs
Arithmetical mean height (Sa)	1.50	4.02
Root mean square height (Sq)	1.84	5.08
Degree the roughness shape (Ssk)	0.09	0.13
Kurtosis (SKu)	-0.375	0.1719
Maximum peak height (Sp)	6.67	23.002
Maximum pit height	6.49	20.6

from pregnant women and women who had experienced miscarriages while visiting hospitals and health centers. The sampleswere collected in sterile containers and immediately transported to the laboratory under sterile conditions for microbiological examination.

Isolation and Identification of Microorganisms

Urine sampleswere cultured on blood agar and MacConkey agar plates for bacterial isolates and initial identification of each sCTXle. The sampleswere incubated at 37°C for 24 hours under aerobic conditions and identified by morphological characteristics using Gram staining as a baseline. Final identification was performed using the VITEK C-2bioMérieux system according to the manufacturer's instructions. Susceptibility testing for cefotaxime (CTX) and other antibiotics was performed according to the guidelines of the Clinical and Laboratory Standards Institute (CLSI), and the minimum inhibitory concentration (MIC) values for the tested antibiotics were recorded [19].

Preparation and Identification of Nanoparticles

In this section, chitosan nanoparticles (CSNPs) extracted from shrimp shells were prepared and characterized using atomic force microscopy [20].

Extraction of Chitosan from Shrimp Shells

The shells were collected, washed, dried, and then ground and passed through a sieve to obtain a fine powder. The fine powder was then demineralized with a 1M hydrochloric acid (HCl) solution for 4 hours at room temperature. It was then washed several times with distilled water and left to dry. Protein removal was carried out with a 1M sodium hydroxide (NaOH) solution at 80-90°C with continuous stirring, followed by washing with distilled water. Chitin was then converted to chitosan using a 70% concentrated NaOH solution at 100°C. After this process, it was washed several times with distilled water and then oven-dried at 60°C [21]. Finally, chitosan nanoparticles (CSNPs) were prepared using the direct ion self-assembly method [22]. A 5 mL volume of chitosan solution prepared at a concentration of 0.2 mg/

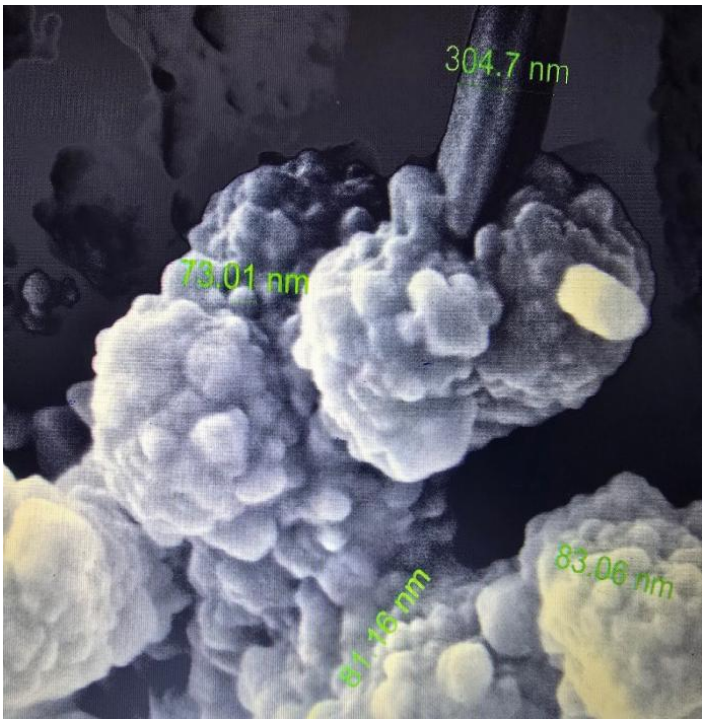

Fig. 4. SEM image illustrating the Cefotaxime loading within the nanocomposite matrix.

ml (dissolved in 1% acetic acid) was transferred into a glass beaker washed with ionized water. Immediately afterward, a 32 µL volume of cefotaxime (CTX) solution was taken and diluted in 20 mL of deionized water to ensure homogeneous distribution of the molecules [23]. The diluted aqueous cefotaxime (CTX) (20 mL) was then added drop by drop and slowly to the chitosan solution (5 mL) under continuous magnetic stirring for 24 hours at room temperature to ensure homogeneity and binding between the antagonist molecules and the amine groups on the surface of the chitosan [24]. The nanoparticles were isolated by centrifugation at 12,000 rpm for 30 minutes at 4°C. The material was separated to measure loading efficiency, while the nanoparticle preCTXitate was washed three times with deionized water and then freeze-dried to obtain pure nano powder.

The material was then separated to measure loading efficiency. 4. Evaluating the Inhibitory Effect of the Nanoparticle.

In this part, the study assessed how the synthesized nanoparticles inhibit three distinct clinical bacterial isolates: Escherichia coli, Klebsiella pneumoniae, and Pseudomonas aeruginosa, which were grown on Mueller-Hinton agar (MHA) and displayed resistance to uncompleted Cefotaxime (CTX). Additionally, the potential synergistic outcomes following the integration of the green nanoparticle were examined. The experimental samples were categorized into three distinct groups, utilizing four replicates per setup, and evaluating two concentrations across the three tested bacterial pathogens. Treatment 1 (T1): This group involved the administration of uncompleted Cefotaxime (CTX) at a minimum inhibitory concentration (MIC) of 16 µg/ml, which was identified via Vitek sensitivity testing for the investigated Escherichia coli, Klebsiella pneumoniae, and Pseudomonas aeruginosa strains [25].Treatment 2 (T2): In this protocol, the specimens were treated with chitosan nanoparticles (CSNPs) at concentrations ranging from 32 to 64 µg/ml for each of the three aforementioned bacterial species. Treatment 3 (T3): This approach utilized chitosan nanoparticles combined with the antibiotic cefotaxime (CTX) at a minimum inhibitory concentration (MIC) of 16 µg/ml and 32 µg/ml against the examined isolates of Escherichia coli, Klebsiella pneumoniae, and Pseudomonas aeruginosa.

RESULTS AND DISCUSSION

The analytical outcomes of the nanocomposite's structural profiling demonstrated that the external layer of the three CSNP nanoparticles exhibited a calculated roughness factor (Sa) and root-mean-square (RMS) based on the relevant equation (Table 1). The arithmetic mean height of this pristine nanocomposite surface (Sa) was equivalent to 1.50 nm (Figs. 1 and 2). Following the incorporation of the antibiotic, this parameter shifted to 4.02, indicating a net variance of 2.52\ nm between the pre- and post-loading phases, which serves as a critical indicator for enhanced performance. A higher degree of variance correlates with a more distinctive crystalline architecture post-loading than prior to the process (Table 1) [27]. Table 1 [28] clarify the surface topography and the subsequent proliferation of protrusions, alongside

Table 2. Antibotic resistance rates for *E. coli* - *Klebsiella pneumoniae* and Pseudomonas aeruginosa.

Antibacterial	Pregnant						Abortions					
Drug	E. coli	Sensitivity	Klebsiella	Sensitivity	Pseudomonas		E. coli		Klebsiella		Pseudomonas	
CEFOTAXIME	G2/2	R	G2/11	R	G3/3	R	G5/4	R	G5/5	R	G5/20	R
	G2/6	R	G2/15	R	G3/9	R	G5/22	R	G5/27	R	G5/23	R
	G2/8	R	G2/21	R	G3/17	R	G5/24	R	G5/31	R	G5/30	R
	G2/10	R					G5/26	R	G5/39	R	G5/50	R
	G2/13	R					G5/29	R	G5/43	R		
	G2/16	R					G5/32	R	G5/46	R		
							G5/34	R				
							G5/36	R				
							G5/37	R				
							G5/40	R				
							G5/42	R				
							G5/45	R				
TOTAL%	(6)100%		(3)100%		(3)100%		(12)100%		(6)100%		(4)100%	

*R = Resistance, S= Sensitive

luminous spots that scatter light. This effect causes the post-loading surface matrix to appear dimmer relative to its initial state.Furthermore, the data validate successful loading by tracking the dimensional growth of these protrusions, where the maximal peak expanded by 6.67\ nm. The structural cavities increased in thickness from 6.49\ nm to 23.002\ nm, while their vertical height extended from 6.49\ nm to 20.6\ nm, confirming a well-distributed loading process. This uniform distribution was verified symmetrically, as detailed in Table 1.

The symmetry of the profile height varies based on the Ssk value: a negative Ssk indicates an elevation distribution concentrated above the average reference plane, whereas a positive value reflects a distribution below it. When Ssk equals zero, the peaks and valleys are uniformly balanced around the central plane.

Prior to drug entrapment, the surface features of the synthesized nanocomposite were investigated using SEM (Fig. 3). A homogenous distribution of spherical-shaped, well-dispersed particles with rough surface characteristics was observed. This elevated roughness is crucial for biomedical systems as it expands the surface area-to-volume ratio, thereby enhancing the matrix capacity for Cefotaxime immobilization. The particle sizes were determined to span a range of 115.4–299.0 nm."

Following the immobilization of cefotaxime, distinct alterations in both surface topography and cluster configuration became evident, as illustrated in Fig. 4. SEM micrographs confirmed the successful integration of the antibiotic onto the nanocomposite matrix, which induced minor particle agglomeration and texture modifications. While the carrier maintained its predominantly spherical cluster morphology, the localized particle dimensions spanned from 73.01 to 304.7 nm. This effective loading efficiency underscores the compatibility and potential of the synthesized matrix as a robust vehicle for targeted drug delivery."

Recent research indicates that elevated resistance levels have been observed in the most common types of bacteria in pregnant women

Table 3. Inhibition zone diameters of *E. coli* following treatment with CS/NPs nanocomposite, both prior to and after incorporating the antibiotic Cefotaxime (CTX).

Treatment	Inhibition zone/mm Concentration/ Ug/ml	mean± standard error	LSD
T1 CTX	C1 (16ug)50µ	0.50±0.577	2.93
	C2(32µg)50µ	2.05±0.816	2.93
	Total	0±.3661.25	2.07
T2 CSNPs	C1(32µg)50µ	6.50±1.291	
	C2(64µg)50µ	15.25±2.630	
	Total	1.885±10.875	
T3 CSNPs/CTX	C1(16/2)50µ	1.708±19.75	
	C2(32/2)50µ	2.217±22.75	
	Total	0.871±21.25	

Table 4. Evaluation of inhibition zone sizes against Klebsiella pneumoniae using CS/NPs nanocomposite before and after the loading of Cefotaxime (CTX) antibiotic.

Treatment	Inhibition zone/mm Concentration/ Ug/ml	mean± standard error	LSD
T1 CTX	C1 (16ug)50µ	0.25 ±0.500	1.51
	C2(32µg)50µ	1.75±0.957	1.61
	Total	1.00±0.35	1.07
T2 CSNPs	C1(32µg)50µ	3.50±1.291	
	C2(64µg)50µ	6.50±1.291	
	Total	5.00±0.681	
T3 CSNPs/CTX	C1(16/2)50µ	7.75±0957	
	C2(32/2)50µ	11.50±1.291	
	Total	9.625±0.750	

and those with urinary tract infections(UTI|), specifically Escherichia coli, Klebsiella pneumoniae, and Pseudomonas aeruginosa, for the antibiotic cefotaxime (CTX). Escherichia coli resistance to cefotaxime (CTX) reached 100%, with a minimum inhibitory concentration (MIC) of 32 µg/ml, as shown in Table 2. Escherichia coli resistance to CTX (cefotaxime) is a critical health issue drive by the inappropriate administration of antimicrobials [29]. Cefotaxime resistance is linked to changes in intracellular cefotaxime (CTX) concentration and diminished cellular permeability [30] in Gram-negative bacteria such as *Escherichia coli*, *Klebsiella pneumoniae*, and *Pseudomonas aeruginosa* exhibits resistance to the antibiotic cefotaxime and possess the capacity to synthesise extended-spectrum beta-lactamase (ESBL) enzymes. These strains also possess resistance mechanisms associated with altered glucose-modified glycolytic pathways, inhibiting glucose breakdown and contributing to increased intracellular glucose accumulation. This leads to

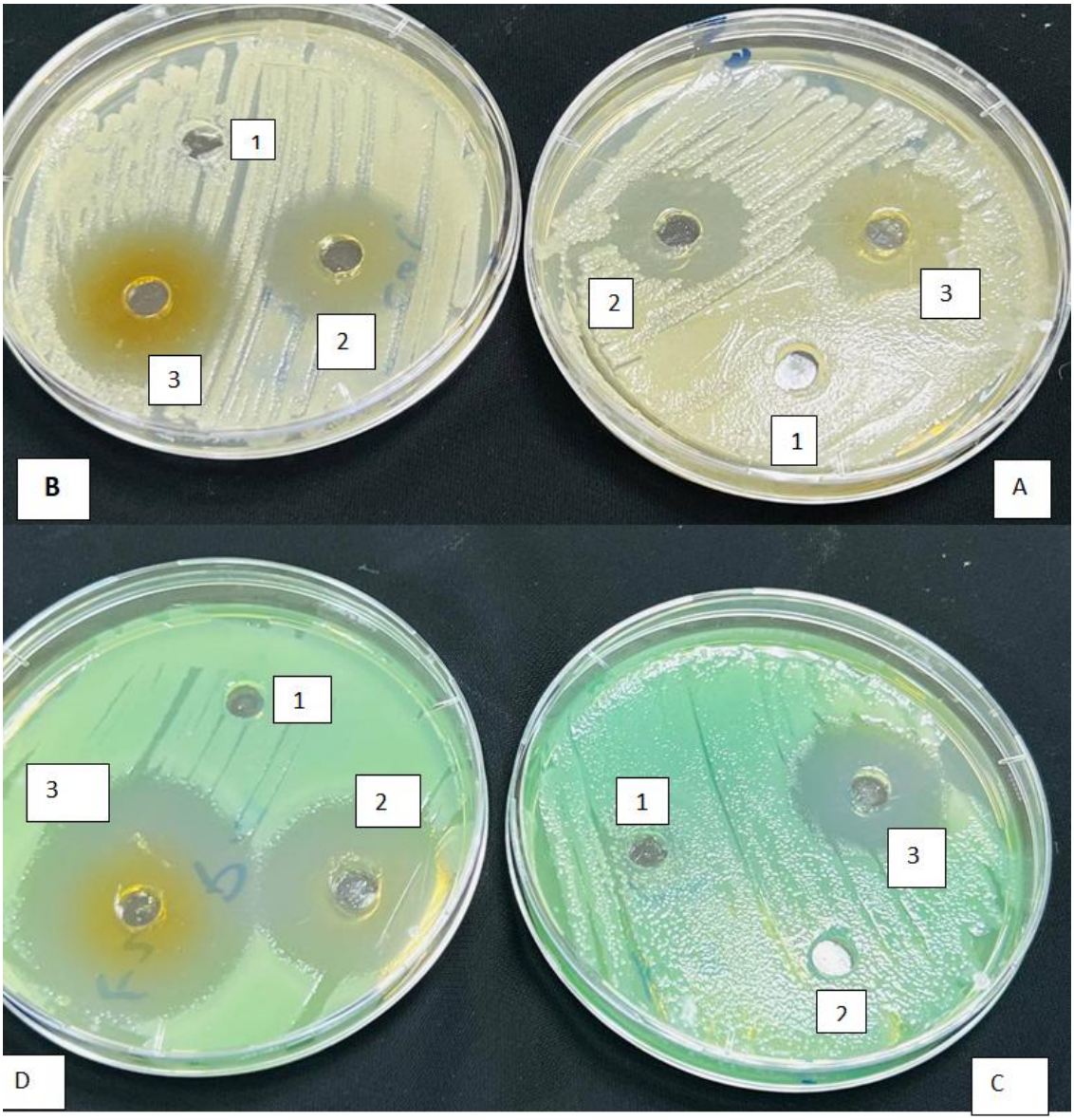

Fig. 5. Comparative analysis of inhibition zone diameters (mm) measured at C1 against the MIC values (µg/mL): (A) *E. coli* below MIC, (B) *E. coli* above MIC, (C) *K. pneumoniae* below MIC, and (D) *K. pneumoniae* above MIC.

genetic mutations and the generation of reactive oxygen species (ROS) [31]. Synergistic treatment combining the antibiotic cefotaxime (CTX) with certain antimicrobial peptides (CTXs) has been shown to reduce the likelihood of resistance development in Escherichia coli, Klebsiella pneumoniae, and Pseudomonas aeruginosa. Treatment with CTX-loaded nanoparticles, such as chitosan nanoparticles, can inhibit bacterial resistance development, particularly against strains that have already developed resistance due to exposure to low concentrations that suppress bacterial growth without eradication. [32] Antibiotic resistance in Escherichia coli, Klebsiella pneumoniae, and Pseudomonas aeruginosa bacteria isolated from infected women has been studied in many previous research studies. Previous studies [33] showed that Escherichia coli, Klebsiella pneumoniae, and Pseudomonas aeruginosa isolates from processed cheeses were associated with high levels of drug resistance (MDP). These results mirror those reported by several studies, including one in Nigeria, which showed many antibiotic-resistant bacterial isolates in women with abortions and urinary tract infections and resistance genes [34].

The results of the current study, shown in Table 3 and Fig. 5, indicate significant differences in the inhibition diameters of E. coli bacteria when treated with the antibiotic and chitosan nanoparticles (Chitosan NPs), and utilizing the antibiotic -loaded nanocomposite (Chitosan NPs/CTX). Treatment with the antibiotic (T1) showed the lowest inhibition diameter at (1.25 ± 0.366) mm, indicating high resistance of the bacterial isolates to Cefotaxime. Treatment with chitosan nanoparticles (T2) showed a significant increase in the inhibition diameter at (10.875 ± 1.885) mm, indicating that the nanoparticles possess inhibitory activity against the studied bacteria. Treatment with the nanocomposite with the antibiotic (T3) achieved the highest inhibition diameter at (21.25 ± 0.871) mm, with significant differences (P≤0.05) compared to all other treatments.

Regarding the effect of concentrations on the inhibition diameter, treatment (T3) at the first concentration (C1) recorded an inhibition diameter of (19.75 ± 1.708) mm, while the inhibition diameter increased at the second concentration (C2) to (22.75 ± 2.217) mm. This indicates a direct relationship between increasing concentration and increasing inhibitory activity of the antibody-loaded nanocomposite. These values also significantly exceeded those recorded in treatment (T2), which reached (6.50 ± 1.291) and (15.25 ± 2.630) mm for the first and second concentrations, respectively. The same was true for treatment (T1) at the first and second concentrations, which were (0.50 ± 0.577) and (2.05 ± 0.816) mm, respectively. These results indicate that loading Cefotaxime onto chitosan nanoparticles enhanced its antibacterial efficacy and increased its ability to inhibit the growth of *E. coli* bacteria.

The results in Table 4 and Fig. 5 showed significant differences in the diameters of inhibition of K. pneumoniae bacteria between the treatment with the antibiotic cefotaxime (CTX), the nano chitosan (Chitosan NPs), and the nanocomposite with the antibiotic (Chitosan NPs/CTX). Treatment with the free antibiotic Cefotaxime (T1) showed the lowest inhibitory activity at concentrations 16 and 32, with an average inhibition diameter of 0.25 ± 0.500 mm for concentration 16 and 1.75 ± 0.957 mm for concentration 2. In contrast, treatment with the chitosan nanoparticle (T2) demonstrated better inhibitory activity than the free antibiotic, with inhibition diameters of 3.50 ± 1.291 mm for concentration 1 and 6.50 ± 1.291 mm for concentration 2. Treatment with the cefotaxime-loaded nanoparticle (T3) showed a clear and significant advantage over the other treatments, recording the highest inhibition diameter values of 7.75 ± 0.957 mm for concentration 1 and 11.50 ± 1.291 mm for concentration 2. As the results show, treatment (T3) at the lower concentration (C1) achieved higher efficacy than all values of free Cefotaxime at both concentrations, as it clearly outperformed treatment (T1). This may be attributed to the ability of nanoparticles to improve the delivery of the antibiotic to bacterial cells and increase its permeability through cell membranes, as well as the synergistic effect between chitosan and Cefotaxime, which contributed to enhancing the sensitivity of K. pneumoniae bacteria and reducing their resistance to the antibiotic.

CONCLUSION

This study demonstrated that urinary tract infection-associated bacteria isolated from pregnant women and women with miscarriage, especially Escherichia coli, Klebsiella pneumoniae, and Pseudomonas aeruginosa, showed high resistance to cefotaxime, indicating a serious

therapeutic challenge. Free cefotaxime produced very limited antibacterial activity, confirming the reduced effectiveness of this antibiotic against resistant clinical isolates. Chitosan was successfully extracted from shrimp shells and converted into chitosan nanoparticles, which were then loaded with cefotaxime. AFM and SEM analyses confirmed successful nanoparticle formation and drug loading through clear changes in surface roughness, topography, and particle morphology. These findings support the suitability of chitosan nanoparticles as an effective drug-delivery carrier. Biological testing showed that chitosan nanoparticles alone had measurable antibacterial activity, whereas cefotaxime-loaded chitosan nanoparticles produced significantly greater inhibition against the tested resistant bacteria than either free cefotaxime or unloaded nanoparticles. The strongest effect was observed against E. coli, with inhibitory activity increasing at higher concentrations. Overall, cefotaxime-loaded chitosan nanoparticles appear to be a promising strategy for improving antibacterial efficacy against resistant UTI pathogens. This nanocomposite may offer an alternative approach for controlling antibiotic-resistant infections, although further in vivo, toxicity, and mechanistic studies are needed before clinical application.

CONFLICT OF INTEREST

The authors declare that there is no conflict of interests regarding the publication of this manuscript.

REFERENCES

1. Youssef MA, Hamza NM, Hussain KAM. The effect of aqueous extract of Cinnamonum zeylanicum on some biochemical parameters in male white rats in which rheumatoid arthritis is induced. AIP Conference Proceedings: AIP Publishing; 2023. p. 020031.
2. Ahmed VA, Hamad NS, Balaky HM, Ismail PA, Ahmed BS. Early Detection of Miscarriage in Recurrent Pregnancy Loss Using a Novel Urinary Biomarker. Al-Rafidain Journal of Medical Sciences (ISSN 2789-3219). 2025;9(2):182-187.
3. Ali A, Elfituri A, Doumouchtsis SK, Zini ME, Jan H, Ganapathy R, et al. Managing couples with recurrent miscarriage: A narrative review and practice recommendations. International Journal of Gynecology and Obstetrics. 2023;164(2):499-503.
4. Garmendia JV, De Sanctis CV, Hajdúch M, De Sanctis JB. Microbiota and Recurrent Pregnancy Loss (RPL); More than a Simple Connection. Microorganisms. 2024;12(8):1641.
5. Chaudhri N, Masud M, Shehzad MN, Kumar J, Qureshi MA, Sarwar N. Antimicrobial Susceptibility and Resistance Patterns in Urine Cultures - A Single-Center Experience. Journal of Rawalpindi Medical College. 2020:74-79.
6. Eidan ZA, Shani WS, Almazini MA-I. Identification of bacterial isolates in urinary tract infections patients of Basrah province. European Journal of Clinical and Experimental Medicine. 2025;23(1):205-214.
7. Al-Awkally NAM, Ibrahim HK, Ali MD, Muthanna FM, Al-Awkally AM, Yousuf A. Study of antibiotic sensitivity pattern in urinary tract infection. International journal of health sciences. 2022:8896-8913.
8. Haddad JM, Ubertazzi E, Cabrera OS, Medina M, Garcia J, Rodriguez-Colorado S, et al. Latin American consensus on uncomplicated recurrent urinary tract infection—2018. International Urogynecology Journal. 2019;31(1):35-44.
9. Hanoon N. Prevalence of urinary tract infections among pregnant women in Iraq: meta-analysis study. University of Thi-Qar Journal of Science. 2024;11(2):1-7.
10. Laza R, Luput-Andrica I-M, Marinescu A-R, Cut T-G, Herlo A, Saizu A-E, et al. Clinical Predictors and Pathogen Resistance Dynamics in Hospitalized Patients with Urinary Tract Infections: A 2025 Institutional Study. Microorganisms. 2026;14(4):916.
11. Paul P, Kolesinska B, Sujka W. Chitosan and Its Derivatives - Biomaterials with Diverse Biological Activity for Manifold Applications. Mini-Rev Med Chem. 2019;19(9):737-750.
12. Jafernik K, Ładniak A, Blicharska E, Czarnek K, Ekiert H, Wiącek AE, et al. Chitosan-Based Nanoparticles as Effective Drug Delivery Systems—A review. Molecules. 2023;28(4):1963.
13. Duolikun T, Lai CW, Bin Johan MR. Agricultural waste-based bionanocomposites in tissue engineering and regenerative medicine. Bionanocomposites in Tissue Engineering and Regenerative Medicine: Elsevier; 2021. p. 499-506. http://dx.doi.org/10.1016/b978-0-12-821280-6.00009-x
14. Mawazi SM, Kumar M, Ahmad N, Ge Y, Mahmood S. Recent Applications of Chitosan and Its Derivatives in Antibacterial, Anticancer, Wound Healing, and Tissue Engineering Fields. Polymers. 2024;16(10):1351.
15. Hussain KAM, Al-Rubaiy SSH, Al-awad HAR. Green synthesis and characterization of a nanocomposite Petroselinum crispum (PcNps) and evaluation of its effect on the inhibition of Pseudomonas aeruginosa before and after loading the antibiotic erythromycin. Journal of Applied and Natural Science. 2025;17(2):574-581.
16. Al-Karawi RH, Al-Safy AH, Hussain KAM. Study the Effect of Ibuprofen Loaded with Green Nanocomposite on Blastocyst Implantation in Female Albino Rats. Lecture Notes in Networks and Systems: Springer Nature Singapore; 2025. p. 531-547. http://dx.doi.org/10.1007/978-981-96-3244-2_42
17. Shaheen AA, M. Hussain KA, Al-Safy AH. Preparation and characterization of nanocomposite from fresh green Asparagus Officinalis L. Stems and study of its biological efficacy in treating polycystic ovary syndrome induced by metformin suppository. ASEAN Journal of Psychiatry. 2024:01-09.
18. Shneen SY, Hussain MIJKAM. Green Biosynthesis of Silver Nanoparticles from Moringa oleifera Leaf Extracts and Their Efficacy Against the Pulse Beetle, Callosobruchus maculatus. BIOPESTICIDES INTERNATIONAL. 2024;20(01):83.
19. Malik S, Muhammad K, Waheed Y. Emerging Applications of Nanotechnology in Healthcare and Medicine. Molecules. 2023;28(18):6624.
20. Younes I, Rinaudo M. Chitin and Chitosan Preparation from Marine Sources. Structure, Properties and Applications.

Mar Drugs. 2015;13(3):1133-1174.
21. Hossain MS, Iqbal A. Production and characterization of chitosan from shrimp waste. Journal of the Bangladesh Agricultural University. 2014;12(1):153-160.
22. Al-Nemrawi N, Wahsheh Y, Alzoubi KH. Transdermal Delivery of Methotrexate Loaded in Chitosan Nanoparticles to Treat Rheumatoid Arthritis. Curr Drug Del. 2024;21(3):451-460.
23. Sorasitthiyanukarn FN, Muangnoi C, Rojsitthisak P, Rojsitthisak P. Chitosan-alginate nanoparticles as effective oral carriers to improve the stability, bioavailability, and cytotoxicity of curcumin diethyl disuccinate. Carbohydr Polym. 2021;256:117426.
24. Capek I. Smart therapeutic-polymer-loaded silica nanomaterials. Nanomedicine. Polymer-Plastics Technology and Materials. 2020;59(11):1139-1147.
25. Raza M, Kanwal Z, Rauf A, Sabri A, Riaz S, Naseem S. Size- and Shape-Dependent Antibacterial Studies of Silver Nanoparticles Synthesized by Wet Chemical Routes. Nanomaterials. 2016;6(4):74.
26. Mansoor MS, Raza N, Bibi F, Mumtaz M, Abbas A, Haider F, et al. Advances in Chitosan Nanoparticles: A Comprehensive Review of Properties, Synthesis, Characterization, Multidisciplinary Applications, and Future Perspectives. J Appl Polym Sci. 2026;143(33).
27. Czifra Á, Goda T, Garbayo E. Surface characterisation by parameter-based technique, slicing method and PSD analysis. Measurement. 2011;44(5):906-916.
28. Prediction of Surface Roughness Parametres by New Experimentally Validated Modelling Algorithm under Abrasive Condition. Acta Polytechnica Hungarica. 2016;13(7).
29. Wu D, Ding Y, Yao K, Gao W, Wang Y. Antimicrobial Resistance Analysis of Clinical Escherichia coli Isolates in Neonatal Ward. Frontiers in Pediatrics. 2021;9.
30. Maher C, Maharjan R, Sullivan G, Cain AK, Hassan KA. Breaching the Barrier: Genome-Wide Investigation into the Role of a Primary Amine in Promoting E. coli Outer-Membrane Passage and Growth Inhibition by Ampicillin. Microbiology Spectrum. 2022;10(6).
31. Dengler Haunreiter V, Tarnutzer A, Bär J, von Matt M, Hertegonne S, Andreoni F, et al. C-di-AMP levels modulate Staphylococcus aureus cell wall thickness, response to oxidative stress, and antibiotic resistance and tolerance. Microbiology Spectrum. 2023;11(6).
32. Kosaristanova L, Rihacek M, Sucha F, Milosavljevic V, Svec P, Dorazilova J, et al. Synergistic antibacterial action of the iron complex and ampicillin against Staphylococcus aureus. BMC Microbiol. 2023;23(1).
33. Kasem N, Ashmawy M, Elsherbini M, Abdelkhalek A. Antimicrobial resistance and molecular genotyping of Escherichia coli and Staphylococcus aureus isolated from some Egyptian cheeses. Journal of Advanced Veterinary and Animal Research. 2021;8(2):246.
34. Adekunle OC, Fatila AJF, Ojedele R, Odewale G. Detection of Antibiotic Resistance Genes in Some Multiple Antibiotic Resistant E. coli from Apparently Healthy Pregnant Women. Microbiology Research Journal International. 2020:23-31.